

THESES OF DOCTORAL (PH.D.) DISSERTATION

Domonkos Attila Tasi

***Ab initio* characterization and dynamics of S_N2
reactions involving polyatomic nucleophiles**

Supervisor:

Dr. Gábor Czakó

associate professor

Doctor of the Hungarian Academy of Sciences



University of Szeged

Faculty of Science and Informatics

Department of Physical Chemistry and Materials Science

Doctoral School of Chemistry

MTA-SZTE Lendület Computational Reaction Dynamics

Research Group

Szeged

2023

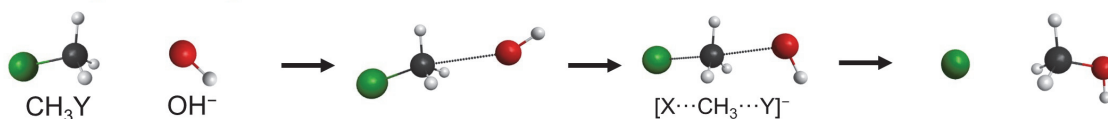
1 Introduction and aims

Bimolecular nucleophilic substitution (S_N2) is an elemental reaction, which has been thoroughly investigated in gas phase utilizing experimental and theoretical methods, as well. In case of a prototype $X^- + CH_3Y \rightarrow CH_3X + Y^-$ S_N2 reaction, the traditional Walden-inversion mechanism occurs *via* a typically submerged $[X\cdots CH_3\cdots Y]^-$ penta-covalent transition state, which connects two pre- and post-reaction ion-dipole and/or hydrogen-bonded minima. Besides inversion, retention can also occur by two pathways: front-side attack and double inversion. Front-side attack proceeds through a high-energy $[XYCH_3]^-$ transition state, while double inversion, unveiled by Szabó and Czakó in 2015, takes place along a lower-energy route: The first step is a proton-abstraction induced inversion *via* the $[XH\cdots CH_2Y]^-$ transition state, and the second step is the conventional Walden-inversion mechanism. By the 2010s, it has become evident, that the picture of the S_N2 reactions is much more complex, than previously assumed. Depending on the reactants and the reaction conditions, the classical Walden inversion can eventuate *via* several direct and indirect mechanisms, such as: ion-dipole complex formation, roundabout, stripping, *etc.*, as shown in Figure 1. Besides S_N2 , proton abstraction can also occur, leading to the $CH_2Y^- + HX$ products. Furthermore, in case of the $X^- + CH_3(CH_2)_nY$ [$n = 1, 2, \dots$] reactions, bimolecular elimination ($E2$) is also a possible pathway, which results in $Y^- + HX + C_{n+1}H_{2n+2}$.

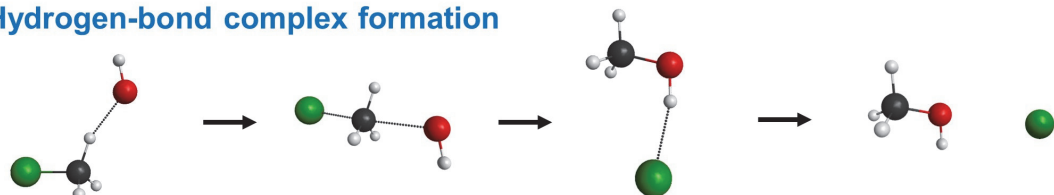
The quasi-classical trajectory (QCT) simulation is one of the most preferred methods to theoretically characterize the dynamics of a chemical reaction. In the course of the direct dynamics computation, the potential energy and the gradient are obtained by an electronic structure program at each configuration of the system, thus, less reliable low-level methods can be utilized due to the significant number of calculations. On the other hand, the potential energy surface (PES) of the reaction can be represented with an analytical function providing a computationally more efficient approach. In that case, the primary aim is to develop the PES as accurate as possible. For this purpose, Gyóri and Czakó, developed the so-called ROBOSURFER program package, which allows us to construct the PES of a chemical reaction automatically. Since then, numerous PESs have been developed for reactive systems using the ROBOSURFER program: $Cl + C_2H_6$, $F^- + CH_3Br$, $F^- + NH_2Cl$, $F^- + CH_3CH_2Cl$, $OH + C_2H_6$, *etc.*

Walden-inversion pathways

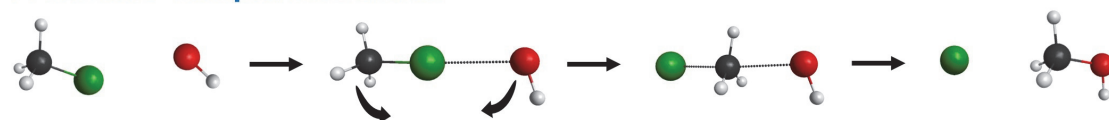
Ion-dipole complex formation



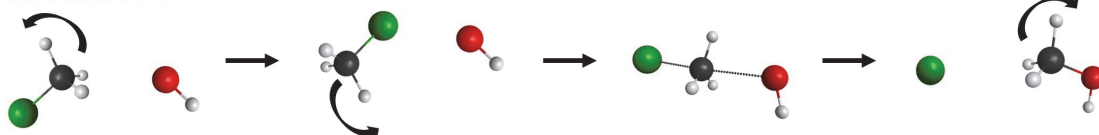
Hydrogen-bond complex formation



Front-side complex formation



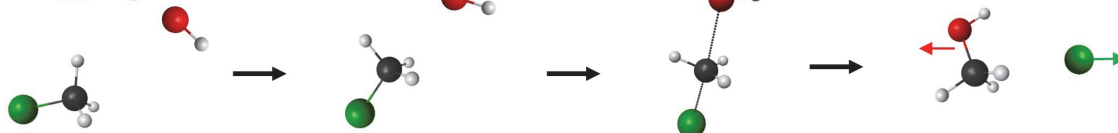
Roundabout



Rebound

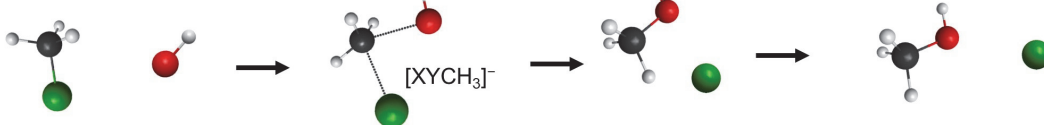


Stripping

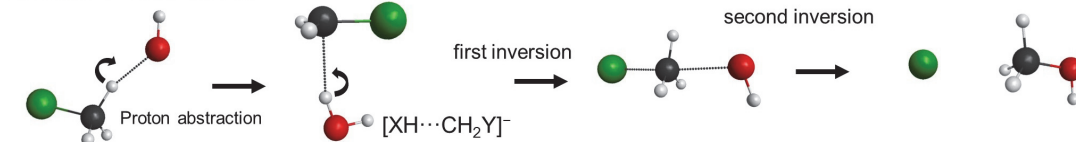


Retention pathways

Front-side attack



Double inversion



blue: indirect red: direct

Figure 1. The possible direct and indirect mechanisms of the $\text{OH}^- + \text{CH}_3\text{Y}$ [$\text{Y} = \text{F}, \text{Cl}, \text{Br}$ and I] $\text{S}_{\text{N}}2$ reactions denoting the structures of the transition states of Walden inversion, front-side attack and double inversion.

Moving beyond the conventional six-atomic S_N2 reactions between halide ions and methyl halides, the subsequent crucial challenge is to analyse reactions containing other, two- or three-atomic nucleophiles. Hence, during my doctoral work, I focused on the S_N2 reactions between OH^- , CN^- , SH^- , NH_2^- and PH_2^- ions and CH_3Y [$\text{Y} = \text{F}, \text{Cl}, \text{Br}$ and I]. One of my objectives was to characterize the stationary points with respect to the previously unexplored double-inversion and front-side attack pathways. In case of OH^- , the reaction with $\text{CH}_3\text{CH}_2\text{Y}$ was also planned to consider. Out of the aforementioned reactions, the most studied is $\text{OH}^- + \text{CH}_3\text{Y}$: Noteworthy that, Hase and co-workers preformed direct dynamics simulations on the $\text{OH}^- + \text{CH}_3\text{F}$ reaction, and revealed that the reaction avoids the hydrogen-bonded $\text{CH}_3\text{OH}\cdots\text{F}^-$ deep minimum in the exit channel. It is worth highlighting that, for the dynamical investigation of the $\text{OH}^- + \text{CH}_3\text{I}$ reaction, the combination of the crossed-beam and velocity imaging techniques were employed by Wester and co-workers, supplemented with direct dynamics simulations. Motivated by these findings, my goal was to develop high-level analytical global PESs for $\text{OH}^- + \text{CH}_3\text{F}/\text{CH}_3\text{I}$ in order to investigate the dynamics of the reactions with the QCT method. Furthermore, I also aimed to perform the first high-level dynamical characterization of the polyatomic $\text{NH}_2^- + \text{CH}_3\text{I}$ reaction.

2 Methods

For the *ab initio* geometry optimizations, energy and frequency calculations of the stationary points, the MOLPRO program was used, and the post-CCSD(T) effects were determined by the MRCC program package interfaced to MOLPRO. The structures and frequencies were computed at the CCSD(T)-F12b/aug-cc-pVTZ level of theory, and the energies were obtained by single-point calculations using the CCSD(T)-F12b method with the aug-cc-pVQZ basis sets at these geometries. For the $\text{OH}^- + \text{CH}_3\text{Y}$ reactions, post-CCSD(T) effects and core correlations were considered, as well as, for $\text{CN}^- + \text{CH}_3\text{Y}$, where relativistic effects were also determined. For Br and I, relativistic small-core effective core potentials and the corresponding pseudo-potential basis sets were applied. The PES developments of the $\text{OH}^- + \text{CH}_3\text{F}/\text{CH}_3\text{I}$ and $\text{NH}_2^- + \text{CH}_3\text{I}$ reactions were performed by the ROBOSURFER program connected to MOLPRO, and the QCT simulations were carried out by in-house programs. The analyses of the QCT results were performed by my own FORTRAN 90 program codes and AWK scripts.

3 Results

Characterization of the stationary points of the $X^- + CH_3Y$ S_N2 reactions [$X = OH^-$, CN^- , SH^- , NH_2^- and PH_2^- , $Y = F$, Cl , Br and I] and the $OH^- + CH_3CH_2Y$ [$Y = F$, Cl , Br and I] S_N2 and $E2$ reactions (T1–T3)

T1. The comparison of the $OH^- + CH_3Y$ and $OH^- + CH_3CH_2Y$ [$Y = F$, Cl , Br and I] reactions was carried out utilizing benchmark *ab initio* methods, and based on their energy profiles, the S_N2 pathways were found to be greatly comparable.

Both reaction-types involve submerged Walden-inversion pathway, hydrogen-bonded global minimum at the product channel, possible low-energy double-inversion pathway resulting in retention of the initial configuration and in case of $Y = I$, stable front-side complex formation can be identified. It was also concluded that the S_N2 pathway of $OH^- + CH_3CH_2Y$ is thermodynamically more favoured than the competitive $E2$, however, considering zero-point energies, the anti- $E2$ path becomes more preferred kinetically. It should be noted that, for the $OH^- + CH_3Y$ reactions, the post-CCSD(T) and core correlation effects were investigated, as well. Moreover, for $OH^- + CH_3CH_2Y$, several reaction enthalpies of other possible pathways were determined, and the calculated data were in excellent agreement with the "experimental" results obtained from the Active Thermochemical Tables.

T2. Benchmark characterization of the S_N2 reactions between the ambident CN^- and methyl halides revealed that the C–C-bond-forming S_N2 reactions are thermodynamically more preferred than the C–N case, while the kinetic preference for the former is not as pronounced.

The cyanide ion has two reactive centers, therefore, for $CN^- + CH_3Y$, two possible S_N2 reactions can occur, forming the $CH_3CN + Y^-$ and $CH_3NC + Y^-$ products. In contrast to the $OH^- + CH_3Y/CH_3CH_2Y$ S_N2 reactions, the double-inversion, as well as, the front-side attack pathways proceed *via* a higher-energy pathway. However, similarly to $OH^- + CH_3Y/CH_3CH_2Y$, in the reactant and product channels, various hydrogen-bonded, halogen-bonded and ion-dipole complexes are located, which may signify probable impact on the dynamics. Furthermore, the reaction enthalpies of the other non- S_N2 reactions were found to be endothermic.

T3. The high-level *ab initio* description of the PESs of the SH^- , NH_2^- and $\text{PH}_2^- + \text{CH}_3\text{Y}$ [$\text{Y} = \text{F}, \text{Cl}, \text{Br}$ and I] $\text{S}_{\text{N}}2$ reactions confirms that notable agreement can be observed in the energy profiles of the $\text{S}_{\text{N}}2$ reactions with the same leaving group.

Among the $\text{S}_{\text{N}}2$ reactions examined in the thesis, the most exothermic is $\text{NH}_2^- + \text{CH}_3\text{I}$, and the only endothermic is $\text{SH}^- + \text{CH}_3\text{F}$. In cases of $\text{OH}^-/\text{NH}_2^-/\text{PH}_2^- + \text{CH}_3\text{I}$ and $\text{NH}_2^- + \text{CH}_3\text{Br}$, instead of the traditional Walden-inversion transition state, a reactant-like transition state is located in the entrance channel. Regarding the retention pathways, typically the transition states of double inversion are situated below than that of front-side attack, moreover for $\text{NH}_2^- + \text{CH}_3\text{Y}$ [$\text{Y} = \text{Cl}, \text{Br}$ and I], as well as, for $\text{OH}^- + \text{CH}_3\text{I}$, the barrier of double inversion vanishes.

QCT study of the dynamics of the $\text{OH}^- + \text{CH}_3\text{F}/\text{CH}_3\text{I}$ and $\text{NH}_2^- + \text{CH}_3\text{I}$ reactions (T4–T7)

T4. For the $\text{OH}^- + \text{CH}_3\text{I}$ reaction, several PESs were constructed at different levels of theory using the ROBOSURFER program package in order to identify the most suitable *ab initio* method for PES development.

Global analytical PESs have been developed for the reactions of $\text{OH}^- + \text{CH}_3\text{F}/\text{CH}_3\text{I}$ and $\text{NH}_2 + \text{CH}_3\text{I}$ utilizing the in-house ROBOSURFER program package. The procedure of the development was devised for the $\text{OH}^- + \text{CH}_3\text{I}$ reaction, and a similar process was employed for $\text{OH}^- + \text{CH}_3\text{F}$ and $\text{NH}_2^- + \text{CH}_3\text{I}$. Throughout the $\text{OH}^- + \text{CH}_3\text{I}$ case, numerous *ab initio* methods were assessed, and eight different PESs were constructed to examine the influence of the various levels of theory on the reaction dynamics. In conclusion, it was concluded that a composite method based on the Brueckner coupled cluster approach is the best-suited candidate for PES development.

To acquire a more thorough insight of the $\text{OH}^- + \text{CH}_3\text{F}/\text{CH}_3\text{I}$ and $\text{NH}_2 + \text{CH}_3\text{I}$ reactions, high-level *ab initio* methods were employed to explore the stationary points of the proton-abstraction channel. In order to provide a detailed dynamical characterization of the reactions, QCT simulations were performed on the constructed PESs at various collision energies.

T5. The dynamics of the $\text{OH}^- + \text{CH}_3\text{I}$ reaction was explored using the QCT method showing a pleasant agreement with the experiment. For proton abstraction, the dominance of the direct stripping mechanism was found, whereas the $\text{S}_{\text{N}}2$ channel displayed a relatively indirect character.

With the crossed-beam results at hand, a comprehensive theoretical–experimental study on the dynamics of the $\text{OH}^- + \text{CH}_3\text{I}$ reaction was presented. Dynamical simulations exposed 11 distinct reaction channels, and experimentally three product ions (I^- , CH_2I^- and $[\text{I}\cdots\text{H}_2\text{O}]^-/[\text{I}\cdots\text{OH}]^-$) were detected. The calculated QCT branching ion ratios, product scattering angle, and internal energy distributions are in good accordance with the measured data. While the direct dynamics results reported earlier qualitatively agree with our computations, however, our QCT investigation shows a significantly better correspondence with the experimental data providing an in-depth understanding of the dynamics of the $\text{OH}^- + \text{CH}_3\text{I}$ reaction.

T6. Nearly 1 million QCT simulations were carried out for the $\text{OH}^- + \text{CH}_3\text{F}$ reaction considering a wide range of collision energy, and our trajectories uncovered a novel, exothermic oxide ion substitution leading to the unexpected products of HF and CH_3O^- .

During this so-called indirect oxide ion substitution, firstly, the traditional Walden inversion occurs, then the system gets trapped in the $\text{CH}_3\text{OH}\cdots\text{F}^-$ region, where afterwards, the F^- removes the proton from the hydroxyl group of CH_3OH . It was demonstrated that this unusual path primarily takes place at lower collision energies, since the $\text{S}_{\text{N}}2$ channel has a more dominant direct character at higher collision energies, allowing the reaction to avoid the hydrogen-bonded deep global minimum. For a more accurate understanding of the role of the $\text{CH}_3\text{OH}\cdots\text{F}^-$ minimum, the $\text{S}_{\text{N}}2$ reactions proceeding through this deep well were distinguished, and the lifetime of the complex was determined at certain cases. Within the framework of the detailed dynamics investigation, all feasible reaction pathways and their cross sections were obtained, and the product internal and relative translational energy, as well as the scattering angle distributions of the $\text{S}_{\text{N}}2$, proton abstraction and oxide ion substitution were also analysed. Highlighting the significance of this novel oxide ion substitution, it should be noted that analogous post-reaction proton-transfer processes can also occur in other reactions, as well: The most promising nominee is $\text{SH}^- + \text{CH}_3\text{F}$, where the corresponding sulfide ion substitution is thermodynamically more preferred than the $\text{S}_{\text{N}}2$ channel.

T7. A high-level dynamical characterization of the eight-atomic $\text{NH}_2^- + \text{CH}_3\text{I}$ reaction was performed for the first time, and our computations unveiled two novel retention pathways for the $\text{S}_{\text{N}}2$ channel.

The QCT simulations revealed that the indirect character of the $\text{S}_{\text{N}}2$ pathway becomes more dominant at higher collision energies facilitating the formation of the vibrationally excited $[\text{CH}_3\cdots\text{NH}_2]$ complexes. At these complexes, the rotation of the CH_3 group is possible promoting two unconventional $\text{S}_{\text{N}}2$ retention pathways. It should be also highlighted that these unusual routes are the most dominant $\text{S}_{\text{N}}2$ retention paths for $\text{NH}_2^- + \text{CH}_3\text{I}$. Moreover, in contrast to the $\text{OH}^- + \text{CH}_3\text{F}/\text{CH}_3\text{I}$ reactions, notable iodine abstraction can be observed, leading to the generation of the $\text{CH}_3 + [\text{NH}_2\cdots\text{I}]^-$ products.

4 Publications covered in the thesis

Hungarian Scientific Bibliography (MTMT) identifier: 10062677

1. **D. A. Tasi***, T. Michaelsen, R. Wester, G. Czakó*: *Quasi-classical trajectory study of the $\text{OH}^- + \text{CH}_3\text{I}$ reaction: Theory meets experiment.* Phys. Chem. Chem. Phys., 25, 4005, 2023, IF: 3.945
2. **D. A. Tasi***, G. Czakó*: *Unconventional $\text{S}_{\text{N}}2$ retention pathways induced by complex formation: High-level dynamics investigation of the $\text{NH}_2^- + \text{CH}_3\text{I}$ polyatomic reaction.* J. Chem. Phys., 156, 184306, 2022, IF: 4.304
3. Z. Kerekes, **D. A. Tasi**, G. Czakó*: *$\text{S}_{\text{N}}2$ reactions with an ambident nucleophile: A benchmark ab initio study of the $\text{CN}^- + \text{CH}_3\text{Y}$ [$\text{Y} = \text{F}, \text{Cl}, \text{Br}, \text{I}$] systems.* J. Phys. Chem. A, 126, 889, 2022, IF: 2.944
4. **D. A. Tasi***, G. Czakó*: *Uncovering an oxide ion substitution for the $\text{OH}^- + \text{CH}_3\text{F}$ reaction.* Chem. Sci., 12, 14369, 2021, IF: 9.969
5. **D. A. Tasi***, C. Tokaji, G. Czakó*: *A benchmark ab initio study of the complex potential energy surfaces of the $\text{OH}^- + \text{CH}_3\text{CH}_2\text{Y}$ [$\text{Y} = \text{F}, \text{Cl}, \text{Br}, \text{I}$] reactions.* Phys. Chem. Chem. Phys., 23, 13526, 2021, IF: 3.945
6. G. Czakó*, T. Győri, D. Papp, V. Tajti, **D. A. Tasi**: *First-principles reaction dynamics beyond six-atom systems.* J. Phys. Chem. A, 125, 2385, 2021, IF: 2.944
7. **D. A. Tasi**, T. Győri, G. Czakó*: *On the development of a gold-standard potential energy surface for the $\text{OH}^- + \text{CH}_3\text{I}$ reaction.* Phys. Chem. Chem. Phys., 22, 3775, 2020, IF: 3.676
8. **D. A. Tasi**, Z. Fábrián, G. Czakó*: *Rethinking the $\text{X}^- + \text{CH}_3\text{Y}$ [$\text{X} = \text{OH}, \text{SH}, \text{CN}, \text{NH}_2, \text{PH}_2$; $\text{Y} = \text{F}, \text{Cl}, \text{Br}, \text{I}$] $\text{S}_{\text{N}}2$ reactions.* Phys. Chem. Chem. Phys., 21, 7921, 2019, IF: 3.430
9. **D. A. Tasi**, Z. Fábrián, G. Czakó*: *Benchmark ab initio characterization of the inversion and retention pathways of the $\text{OH}^- + \text{CH}_3\text{Y}$ [$\text{Y} = \text{F}, \text{Cl}, \text{Br}, \text{I}$] $\text{S}_{\text{N}}2$ reactions.* J. Phys. Chem. A, 122, 5773, 2018, IF: 2.641

Σ IF = 37.798

5 Additional publications

10. G. Czakó*, T. Győri, B. Olasz, D. Papp, I. Szabó, V. Tajti, **D. A. Tasi**: *Benchmark ab initio and dynamical characterization of the stationary points of reactive atom + alkane and S_N2 potential energy surfaces*. Phys. Chem. Chem. Phys., 22, 4298, 2020, IF: 3.676
11. **D. A. Tasi***, J. Csontos, B. Nagy, Z. Kónya, G. Tasi: *Comment on “Causation or only correlation? Application of causal inference graphs for evaluating causality in nano-QSAR models” An alternative interpretation of toxicity of metal oxide nanoparticles towards bacteria Escherichia Coli*. Nanoscale, 10, 20863, 2018, IF: 6.970

$$\frac{\sum \text{IF} = 10.646}{\sum \sum \text{IF} = 48.444}$$

6 Talks and posters

1. T. Győri, **D. A. Tasi**, V. Tajti, D. Papp, G. Czakó: *Towards automated potential energy surface development with ROBOSURFER and ManyHF*. Mátrafüred, MTA Material and Molecular Structure Working Group Meeting. 22.10.2022.
2. **D. A. Tasi**, G. Czakó: *Dynamics of the OH⁻ + CH₃F reaction: The oxide ion substitution*. Balatonföldvár, XVI. International Workshop on Quantum Reactive Scattering, 08.09.2022.
3. T. Győri, **D. A. Tasi**, V. Tajti, D. Papp, G. Czakó: *Tools for automated PES development: ROBOSURFER and ManyHF*, Balatonföldvár, XVI. International Workshop on Quantum Reactive Scattering, 05.09.2022.
4. T. Győri, **D. A. Tasi**, V. Tajti, D. Papp, G. Czakó: *Towards automated potential energy surface development with ROBOSURFER and ManyHF*. Stonehill College, Easton, MA, USA, Molecular Interactions and Dynamics – Gordon Research Conference. 12.07.2022. (poster)
5. T. Győri, **D. A. Tasi**, V. Tajti, D. Papp, G. Czakó: *Towards automated potential energy surface development with ROBOSURFER and ManyHF*. Stonehill College, Easton, MA, USA, Molecular Interactions and Dynamics – Gordon Research Conference. 12.07.2022.

6. **D. A. Tasi**, G. Czakó: *Rendhagyó reakcióút $\text{OH}^- + \text{CH}_3\text{F}$ esetén: az oxidion szubsztitúció.* Szeged, KeMoMo-QSAR Symposium, 02.06.2022.
7. **D. A. Tasi**, G. Czakó: *A $\text{OH}^- + \text{CH}_3\text{F}$ reakció dinamikai vizsgálata: az oxidion szubsztitúció.* Online, MTA Reaction Kinetics and Photochemistry Working Group Meeting, 22.10.2021.
8. **D. A. Tasi**, G. Czakó: *Poliatom-poliatom típusú $\text{S}_{\text{N}}2$ reakció dinamikájának vizsgálata: az $\text{NH}_2^- + \text{CH}_3\text{I}$ reakció esete.* Online, MTA Reaction Kinetics and Photochemistry Working Group Meeting, 27.05.2021.
9. **D. A. Tasi**, G. Czakó: *A $\text{OH}^- + \text{CH}_3\text{I}$ reakció potenciálisenergia-felületének fejlesztése és dinamikája különböző kvantumkémiai szinteken.* Mátrafüred, MTA Reaction Kinetics and Photochemistry Working Group Meeting, 07.11.2019.
10. **D. A. Tasi**, G. Czakó: *A $\text{OH}^- + \text{CH}_3\text{I}$ reakció potenciálisenergia-felületének fejlesztése különböző kvantumkémiai szinteken.* Szeged, XLII. Chemistry Lectures, 30.10.2019.
11. **D. A. Tasi**, G. Czakó: *Rethinking fundamental $\text{S}_{\text{N}}2$ reactions.* XXVIII. International Symposium on Molecular Beams, Edinburgh, 24.06.2019. (poster)
12. **D. A. Tasi**, G. Czakó: *Különböző nukleofilek metil-halogenidekkel történő $\text{S}_{\text{N}}2$ reakcióinak elméleti vizsgálata.* Debrecen, I. FKF Symposium, 04.04.2019.
13. **D. A. Tasi**, Z. Fábrián, G. Czakó: *Az $\text{X}^- + \text{CH}_3\text{Y}$ [$\text{X} = \text{OH}, \text{SH}, \text{CN}, \text{PH}_2, \text{NH}_2$; $\text{Y} = \text{F}, \text{Cl}, \text{Br}, \text{I}$] $\text{S}_{\text{N}}2$ reakciók inverziós és retenciós reakcióútjainak nagy pontosságú ab initio feltérképezése.* Veszprém, MTA Reaction Kinetics and Photochemistry Working Group Meeting, 08.11.2018.
14. **D. A. Tasi**, G. Czakó: *A OH^- , SH^- és CN^- metil-halogenidekkel történő $\text{S}_{\text{N}}2$ reakciók potenciálisenergia-felületeinek nagy pontosságú kvantumkémiai vizsgálata.* Szeged, XLI. Chemistry Lectures, 16.10.2018.
15. **D. A. Tasi**, J. Csontos, B. Nagy, Z. Kónya, G. Tasi: *Fém-oxid nanorészecskék E. coli baktériumokra vonatkozó toxicitásának elméleti vizsgálata nano-QSAR modellekkel.* Szeged, KeMoMo-QSAR Symposium, 25.05.2018.
16. **D. A. Tasi**, G. Czakó: *A $\text{OH}^- + \text{CH}_3\text{Y}$ [$\text{Y} = \text{F}, \text{Cl}, \text{Br}, \text{I}$] $\text{S}_{\text{N}}2$ reakciók inverziós és retenciós reakcióútjainak nagy pontosságú ab initio feltérképezése.* Szeged, KeMoMo-QSAR Symposium, 24.05.2018.